Optical Fiber Technology 20 (2014) 24–27

Contents lists available at ScienceDirect

Optical Fiber Technology

www.elsevier.com/locate/yofte

Invited Paper

Strain-insensitive and high temperature fiber sensor based on a Mach–Zehnder modal interferometer

Zhigang Cao, Zhao Zhang, Xiaochun Ji, Tao Shui, Rui Wang, Chenchen Yin, Shenglai Zhen, Liang Lu, Benli Yu *

Key Laboratory of Opto-Electronic Information Acquisition and Manipulation of Ministry of Education, Anhui University, Jiulong Road 111#, Hefei 230601, China

ARTICLE INFO

Article history:
Available online 28 November 2013

Keywords:
Fiber sensor
Modal interferometer
High temperature
Strain-insensitive

ABSTRACT

In this paper, a strain insensitive high temperature fiber sensor based on the modal interferometer is proposed. It is composed of a piece of small-core photosensitive fiber (SCPSF) which is spliced between two pieces of single mode fiber (SMF). Compared to other high temperature fiber sensor based on the modal interferometer, the sensor owns the highest temperature sensitivity of 106.64 pm/°C from 200 °C to 1000 °C. The temperature to strain cross sensitivity of the sensor is low and only 0.00675 °C/με. The reasons for realizing the high temperature sensitivity is also discussed.

1. Introduction

Compared to the electrical sensors, due to its flexibility, immunity to the electromagnetic interference and durability to harsh environments, optical fiber high-temperature sensors are investigated extensively. These sensors are based on different technologies, such as fiber Bragg grating (FBG) [1], long-period fiber gratings [2], special fiber and interferometer-based systems [3]. Recently, all-fiber Mach–Zehnder interferometer (MZI) based on the modal interferometers have attracted great interest in the high temperature measurement for the advantage of compact structure, low cost and easy fabrication [4–9].

In this paper, we present a strain insensitive and high temperature fiber sensor. It is composed of a section of small-core photosensitive fiber (SCPSF) sandwiched between two pieces of single mode fiber (SMF). In the measurement range of 200–1000 °C, compared to other sensors based on the modal interference, the sensor obtains highest sensitivity of 106.64 pm/°C. The strain sensitivity of the sensor is −0.72 pm/με. Therefore, the temperature-strain cross-sensitivity of the sensor is only 0.00675 °C/με, and it can be used as a strain insensitive and high temperature fiber sensor.

2. Principle of operation

The fiber sensor is mainly composed of a segment of SCPSF, as shown in Fig. 1. The diameters of the core/cladding in the SCPSF are 4.2/125 μm. One end of the SCPSF is spliced to the standard single mode fiber (SMF). The core diameter of the SMF is 9.9 μm. Due to the mismatch of the core, the cladding modes in the SCPSF will be excited at the first spliced point and construct the modal interference with the core mode at the other end of the SCPSF, which is spliced to the SMF with the core-offset.

When only the core mode and the lowest-order cladding mode are taken into consideration, the output intensity of the sensor can be expressed as:

$$I = I_1 + I_2 + 2\sqrt{I_1 I_2}\cos\left[\frac{2\pi\left(n_{co}^{eff} - n_{cl}^{eff}\right)L}{\lambda}\right] \quad (1)$$

where I_1 and I_2 are the intensities of the core mode and the cladding mode, λ is the optical wavelength in air, n_{co}^{eff} and n_{cl}^{eff} are the effective indexes of the core mode and cladding mode in the SCPSF, respectively.

The extinction ratio (ER) of the interferometer can be written as [10]:

$$ER = 10\lg\left[(1+\sqrt{I_2/I_1})/(1-\sqrt{I_2/I_1})\right]^2 \quad (2)$$

According to Eq. (2), in order to obtain a higher extinction ratio in the transmission spectrum of the interferometer, the ratio of I_2/I_1 should be closed to 1. If there is no core-offset at the second spliced point, I_1 will be larger than I_2 and the ER will be low. Due to the core-offset, we can decrease I_1 and increase I_2. Thus, the ER can be improved and there will be an optimized value of the core-offset at the spliced point. The relationship between the ER and the core-offset is investigated in the experiment. Using the tunable laser and power meter in the lightwave measurement

* Corresponding author. Fax: +86 0551 63861781.
E-mail address: benliyu@ahu.edu.cn (B. Yu).

1068-5200/$ - see front matter © 2013 Elsevier Inc. All rights reserved.
http://dx.doi.org/10.1016/j.yofte.2013.11.003

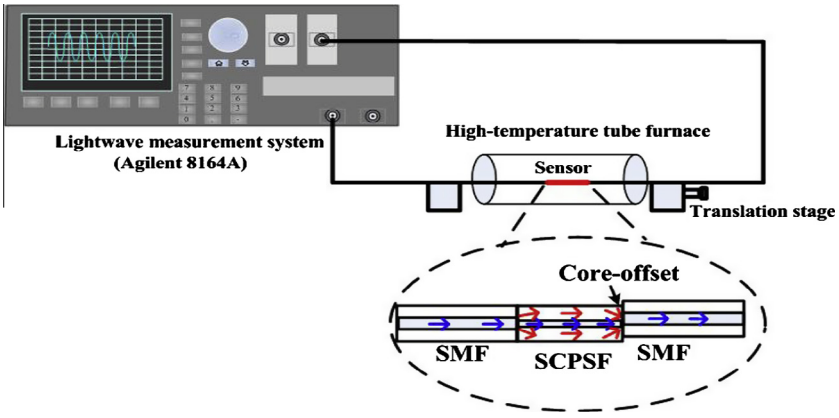

Fig. 1. Schematic configuration of the experimental setup (The inset is the structure of the sensor.)

system (Agilent 8164A), the transmission spectra of the sensor are recorded. The results are shown in Fig. 2. The length of the SCPSF is 5 mm. It can be found that the ER in the transmission spectra increases at first and then decreases as the core-offset increases. When the core-offset is 8 μm, the highest ER is obtained. Besides this, we can also find that the insert loss of the sensor increases all the time due to the increase of the core-offset.

According to Eq. (1), the free spectral range (FSR) of the interfering spectrum can be given as:

$$FSR \approx \lambda^2/\Delta n_{eff} L \tag{3}$$

where $\Delta n_{eff} = n_{co}^{eff} - n_{cl}^{eff}$ is the effective refractive index difference between the core and cladding modes, L is the length of the SCPSF. If the interference intensity reaches its minimum, the phase term in Eq. (1) should be an odd times of π and can be expressed as:

$$\frac{2\pi\Delta n_{eff}}{\lambda} L = (2k+1)\pi \quad (k = 0, 1, 2, 3, \ldots) \tag{4}$$

When strain ε is applied to the SCPSF and ambient temperature ΔT variation occurs, the wavelength shift $\Delta\lambda_d$ of the resonance dip can be expressed as:

$$\frac{\Delta\lambda_d}{\lambda} \approx [(1+p_\varepsilon)\varepsilon + (\alpha+\zeta)\Delta T] \tag{5}$$

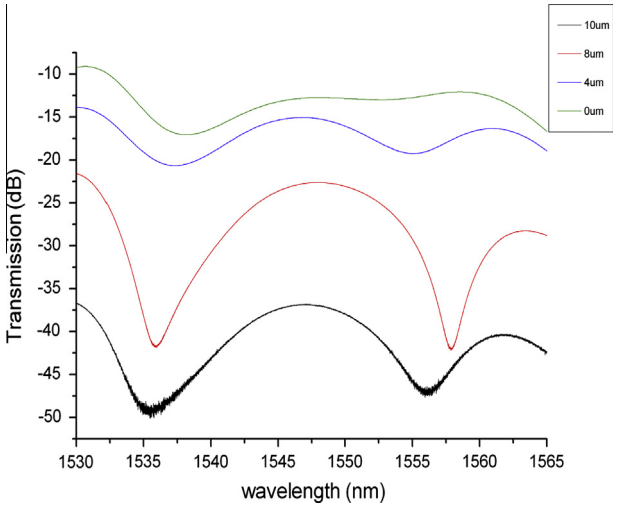

Fig. 2. Experiment with different mismatch splicing distances of 0 μm, 4 μm, 8 μm and 10 μm.

where p_ε is the efficient photoelastic coefficient, $\alpha = \frac{1}{L}\frac{dL}{dT}$ is the thermal expansion coefficient, and $\zeta = \frac{1}{\Delta n_{eff}}\frac{d\Delta n_{eff}}{dT}$ is the efficient thermo-optic coefficient induced by the two interference modes in the SCPSF.

3. Experimental results and discussion

In the experiment, utilizing the sensor, the changes of temperature and strain are measured. Fig. 3 shows the transmission spectra of the sensor with three different length (10 mm, 15 mm and 20 mm) of SCPSF. It can be found that the FSR decrease with the increase of the length of SCPSF. Thus, the experimental results are consistent with the analysis in Eq. (3).

For the temperature measurement, the sensor is placed in the center of a commercial high-temperature tube furnace freely, as shown in Fig. 1. The temperature in the tube can be heated up to 1000 °C. To avoid the temperature fluctuation in the tube, the two ends are plugged by the mullite bricks. Because the length of the constant temperature zone in the tube furnace is 80 mm, the sensor can be heated uniformly. The length of the SCPSF we used at first in the sensor is 5 mm. When the temperature is increased, it can be found that the spectrum shifts to the long wavelength, as shown in Fig. 4(a). In the temperature range of 200–1000 °C, regardless of increase and decrease, the sensor exhibits a good linearity in thermal response, as shown in Fig. 4(b). The result agrees well with the theoretical expectations in Eq. (5). The temperature sensitivity is 106.64 pm/°C and 105.17 pm/°C, respectively. When the length of SCPSF increases from 5 mm to 20 mm, the temperature sensitivity reduces from 106.64 pm/°C to 95.24 pm/°C, as shown in Fig. 4(c). Therefore, the shorter the length of the SCPSF in the sensor is, the higher the temperature sensitivity can be. The thermal expansion coefficient α in Eq. (5) may be used to explain the phenomenon. Because the highest working temperature of our tube furnace is 1000 °C, the temperature sensitivity under higher temperature cannot be measured in this paper now. However, because the small-core photosensitive fiber can be able to withstand high temperature up to 1900 °C, we surmise that the sensor can withstand higher temperature. This will be proved in our next work when higher temperature furnace is obtained.

For the strain measurement, the sensor with 5 mm long SCPSF is mounted on a translation stage of resolution 5 μm. The strain applied to the sensor is from 0 με to 1400 με under the room temperature of 20 °C. Fig. 5 shows the spectrum response to the strain. It can be clearly found that the transmission spectrum of the sensor shifts to the shorter wavelength. Making use of linear curve fitting, the strain sensitivity of the sensor is −0.72 pm/με with a good linearity of 99.8%, as shown in Fig. 6. Therefore, the sensor owns

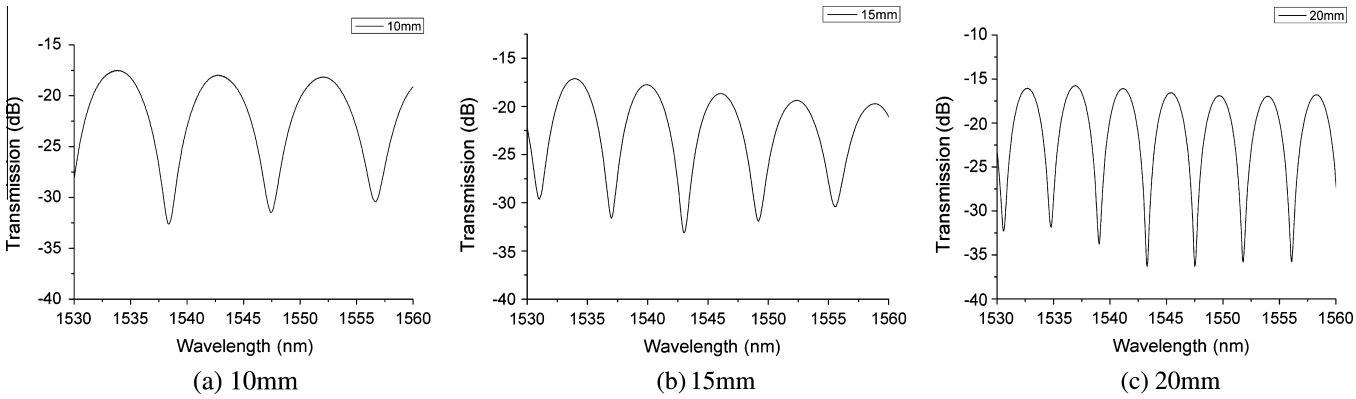

Fig. 3. The transmission spectra of the sensor with different length of the SCPSF.

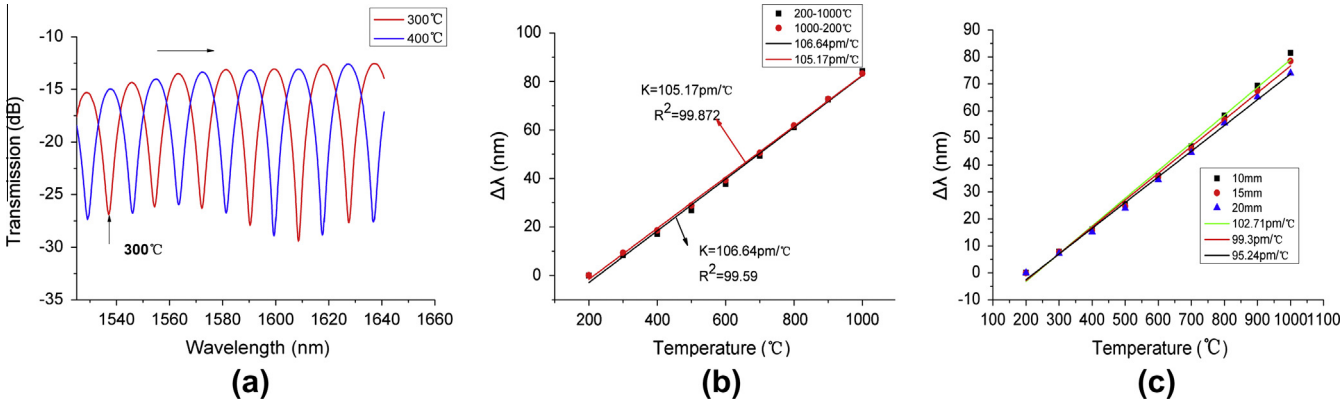

Fig. 4. (a) Spectra responses of the sensor to temperature (300–400 °C), (b) measured wavelength response of the sensor to the temperature, and (c) measured wavelength shifts of the sensor with different length of the TCPO to the temperature.

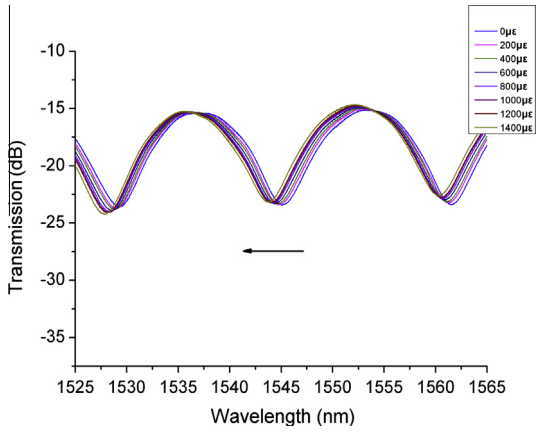

Fig. 5. Transmission spectra versus different strain.

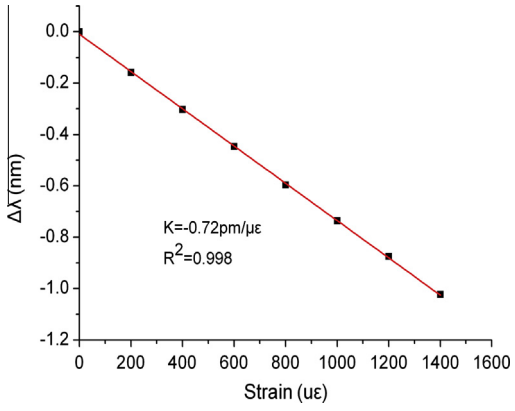

Fig. 6. The spectrum responses of the sensor to the strain.

lower temperature-strain cross-sensitivity 0.00675 °C/με and can be considered as a high temperature fiber sensor with low strain sensitivity.

The temperature sensitivities of different high temperature fiber sensors based on the modal interferometer are presented in Table 1. Compared to the sensors in Table 1, the sensor in this paper owns highest temperature sensitivity.

To explain the high temperature sensitivity and low strain sensitivity of the sensor, the interferences pattern under different temperature and strains are investigated. The wavelength spectra under different temperature and strains are Fourier transformed to obtain the spatial frequency of the interference fringes, as shown in Fig. 7(a) and (b). Fig. 7(a) shows that the power ratios of high order modes increase when temperature is increased. However, when the strain varies from 0 με to 1400 με, Fig. 7(b) shows the power ratios of the higher order cladding modes have slightly changes. This can be explained why the sensor owns the higher temperature sensitivity and lower strain sensitivity. Besides this, a section of small-core photosensitive fiber (SCPSF) is used in the sensor. To improve the photosensitivity of the fiber and keep the single mode operation, GeO_2 and B_2O_3 are doped to the fiber. Compared to the standard single mode fiber, the sensor using the B–Ge codoped fiber can obtain higher temperature sensitivity [2]. It may be the other reason that the sensor owns the higher temperature

Table 1
The temperature sensitivities of different sensors.

Structure type	Temperature sensitivity (pm/°C)	Temperature range (°C)	References
Miniaturized fiber in-line Mach–Zehnder interferometer	46	100–1100	[4]
A dispersion compensation fiber-based interferometer	68.6	25–600	[5]
Miniaturized fiber taper reflective interferometer	20	19–520	[6]
Thin-core single-mode fiber	18.3	25–850	[7]
Waist-enlarged fusion bitaper	70	25–400	[8]
Multimode-single mode-multimode fiber configuration	88	30–900	[9]
Small-core photosensitive fiber	106.64	200–1000	Our paper

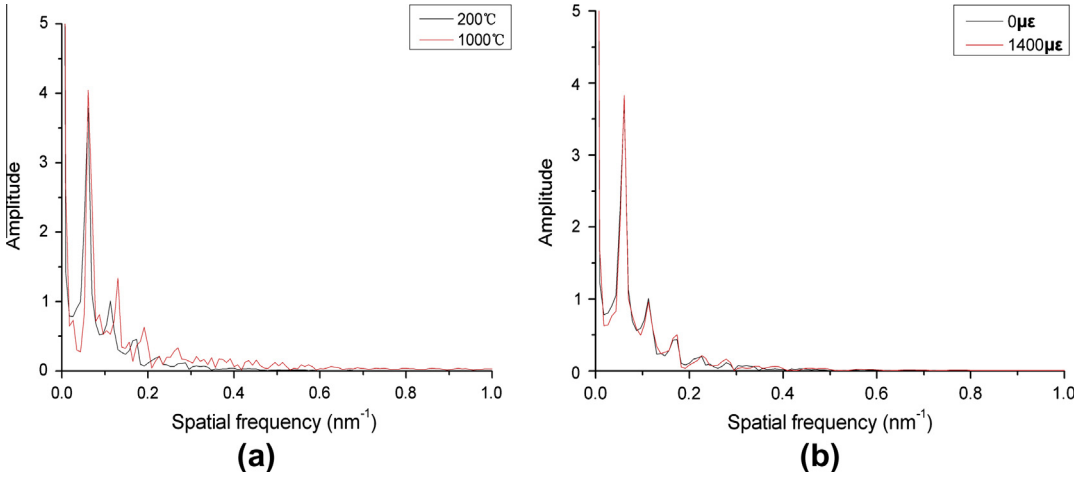

Fig. 7. Spatial frequency spectra by taking the FFT for the transmission spectrum at different (a) temperature and (b) strain.

sensitivity. At last, the core-offset enlarges the changes of the effective refractive index difference of two modes under different temperatures, this may be the third reason.

4. Conclusion

A modal interferometer which is mainly composed of a segment of SCPSF is used as a high temperature sensor for the first time. It has been demonstrated that the sensor owns a high sensitivity of 106.64 pm/°C and low strain sensitivity of −0.72 pm/με. The reasons for realizing the high temperature sensitivity are also analyzed. Compare to the other high temperature sensors which are not based on the modal interferometer, this sensor exhibits the advantages of compact structure, high sensitivity, easy fabrication and low cost.

Acknowledgments

This work was supported by National Natural Science Foundation of China (61307098), the Specialized Research Fund for the Doctoral Program of Higher Education (20113401120002), Educational Commission of Anhui Province of China (KJ2013A021) and the Youth Science Foundation of Anhui University.

References

[1] S. Bandyopadhyay, J. Canning, M. Stevenson, K. Cook, Ultrahigh-temperature regenerated gratings in boron-codoped germanosilicate optical fiber using 193 nm, Opt. Lett. 33 (16) (2008) 1917–1919.
[2] X. Shu, T. Allsop, B. Gwandu, L. Zhang, I. Bennion, High-temperature sensitivity of long-period gratings in B–Ge co-doped fibre, IEEE Photon. Technol. Lett. 13 (8) (2001) 818–820.
[3] Y. Zhu, Z. Huang, F. Shen, A. Wang, Sapphire-fiber-based white light interferometric sensor for high-temperature measurements, Opt. Lett. 30 (7) (2005) 711–713.
[4] Y. Wang, Y. Li, C. Liao, D. Wang, M. Yang, P. Lu, High-temperature sensing using miniaturized fiber in-line Mach–Zehnder interferometer, IEEE Photon. Technol. Lett. 22 (2010) 39–41.
[5] B. Dong, L. Wei, D. Zhou, Miniature high-sensitivity high-temperature fiber sensor with a dispersion compensation fiber based interferometer, Appl. Opt. 48 (33) (2009) 6466–6469.
[6] J. Kou, J. Feng, L. Ye, F. Xu, Y. Lu, Miniaturized fiber taper reflective interferometer for high-temperature measurement, Opt. Express 18 (13) (2010) 14245–14250.
[7] J. Zhu, A. Zhang, T. Xia, S. He, W. Xue, Fiber optic high-temperature sensor based on thin core fiber modal interferometer, IEEE Sens. J. 10 (9) (2011) 1415–1418.
[8] Y. Geng, X. Li, X. Tan, Y. Deng, Y. Yu, High-sensitivity Mach–Zehnder interferometric temperature fiber sensor based on a waist-enlarged fusion bitaper, IEEE Sens. J. 11 (11) (2011) 2891–2894.
[9] L. Nguyen, D. Hwang, S. Moon, D. Moon, Y. Chung, High temperature fiber sensor with high sensitivity based on core diameter mismatch, Opt. Express 16 (15) (2008) 11369–11375.
[10] B. Dong, D. Zhou, L. Wei, W. Liu, J. Lit, Temperature- and phase-independent lateral force sensor based on a core-offset multi-mode fiber interferometer, Opt. Express 16 (23) (2008) 19291–19296.